

---

## **Narrow distillation cuts for an improved characterisation of crude oil: an insight on heteroatoms in heavy fraction molecules**

---

Hendrik Muller\*, Qasim Saleem,  
Emad A. Alawi, Donya A. Alsewdan,  
Imran A.S. Naqvi, Asem H. Saleh and  
Tawfiq A. Rowaished

Research and Development Center,  
Saudi Aramco,  
31311 Dhahran, Saudi Arabia  
Email: hendrik.muller@aramco.com  
Email: qasim.saleem.1@aramco.com  
Email: emad.alawi@aramco.com  
Email: donya.sewdan@aramco.com  
Email: imranahmed.naqvi@aramco.com  
Email: asem.saleh@aramco.com  
Email: tawfiq.rowaished@aramco.com

\*Corresponding author

**Abstract:** A light Arabian crude oil was separated by distillation into 27 fractions, including 25 very narrow distillation cuts, the light ends, and a vacuum residue (VR), which were extensively characterised using standard methods. Overall, the properties matched well with those predicted by H/CAMS software, indicating a successful distillation. Then, quantitative <sup>13</sup>C NMR spectroscopy, SIMDIS, and molecular weight (MW) distribution by mass spectrometry were used to derive an improved correlation between the MW and boiling point for the entire crude oil, in particular for the VR fraction. This allowed determining the mass fractions of sulphur and nitrogen containing compounds across the crude oil boiling range, reaching up to approximately 100% in the VR fraction. The corresponding low abundance of pure hydrocarbon molecules in the VR fraction is important for modelling purposes and processing technologies. [Received: May 3, 2019; Accepted: July 24, 2019]

**Keywords:** petroleum crude oil; distillation; ASTM; APPI time-of-flight mass spectrometry; sulphur content; <sup>13</sup>C NMR.

**Reference** to this paper should be made as follows: Muller, H., Saleem, Q., Alawi, E.A., Alsewdan, D.A., Naqvi, I.A.S., Saleh, A.H. and Rowaished, T.A. (2021) 'Narrow distillation cuts for an improved characterisation of crude oil: an insight on heteroatoms in heavy fraction molecules', *Int. J. Oil, Gas and Coal Technology*, Vol. 26, No. 1, pp.40–59.

**Biographical notes:** Hendrik Muller leads the advanced hydrocarbon characterisation group at the Saudi Aramco R&DC. He obtained his PhD from Muenster University, Germany, in 2004. He is engaged in analytical research and research projects supporting the value chain of Saudi Aramco.

Qasim Saleem is an NMR specialist in the Saudi Aramco R&DC. He obtained his PhD from the University of Toronto, Canada, in 2014. He focuses on supporting analytical research and petrochemical characterisation efforts.

Emad A. Alawi is a senior lab technician at the Saudi Aramco R&DC. He is responsible for crude assays, fractionations and characterisation.

Donya A. Alsewdan is a scientist at the Saudi Aramco R&DC. She obtained her MSc in 2013 from Kent State University, USA. She focuses on method development and downstream support.

Imran A.S. Naqvi is a scientist at the Saudi Aramco R&DC. He obtained his MSc in 1996 from the University of Karachi, Pakistan. He leads the petroleum products testing lab.

Asem H. Saleh is a lab technician at the Saudi Aramco R&DC. He is responsible for the lab scale petroleum crude oil distillation operations.

Tawfiq A. Rowaished is a scientist at the Saudi Aramco R&DC. He obtained his MSc in 2011 from the King Fahd University of Petroleum and Minerals, Saudi Arabia. He leads the crude oil and products testing group.

---

## 1 Introduction

Development and optimisation of oil refining processes can benefit immensely from knowing the physical and chemical properties in the feedstocks and their evolution with the boiling point (BP) (Boduszynski, 1987). The BP distribution of petroleum crude oils is reliably obtained by true boiling point (TBP) determination according to ASTM D-2892 but the procedure is time consuming and unsuitable for a quick estimation of crude oil distillation characteristics (Nedelchev et al., 2011). Already in the late 1980's, Boduszynski et al. published a series of papers on the continuous distribution of petroleum components dependent on the BP. A combination of volatility and solubility separations was used to produce well-defined fractions having progressively higher atmospheric equivalent boiling points (AEBP), followed by, for the time, extensively detailed characterisation. The initial paper reported up to 13 fractions of various crude oils, including Arabian heavy crude oil, and was able to constrain the molecular weights (MWs) to values below 2,000 m/z using field desorption mass spectrometry (FDMS). Furthermore, the distribution of heteroatoms (S, N, O, V, Ni, and Fe) by BP throughout the 13 fractions was described. A second paper reported the distribution of aromatic and aliphatic compounds and the average elemental compositions for the same fractions of two crude oils and added HPLC separation into classes of saturates, multiple aromatics, basic and neutral nitrogen compounds and acidic compounds (Boduszynski, 1988). The combination of HPLC followed by mass spectrometry allowed the distinction between different heteroatom classes, hydrogen deficiency series (Z-numbers), and their carbon number distributions. BP-MW relations factoring the specific gravity, hydrogen to carbon (H/C) ratio, and refractive index were also reported (Altgelt and Boduszynski, 1992). The H/C ratio worked best for whole crude oils and very high boiling atmospheric residue samples. Finally, the crude oil compositional properties were extended to very high AEBP fractions of heavy oils, with implications that those fractions contain

molecules with a multitude of sulphur and nitrogen atoms (Boduszynski and Altgelt, 1992).

Recent reviews on petroleum characterisation by Rodgers and McKenna (2011), Han et al. (2018) and Sama et al. (2018) highlight the advancements in analytical techniques towards the molecular-level understanding of petroleum. Despite these tremendous improvements in analytical capabilities, especially the introduction of such powerful tools as GCxGC and FT-ICR MS, into the field of petroleomics, fractionation of the crude oil into distinct sub-samples is commonly the starting point of analytical strategies. Distillation, often followed by liquid chromatography separations, is thereby the most prevalent means to reduce compositional complexity. For example, three vacuum gas oil distillation fractions (295–319°C, 319–456°C, and 456–543°C) were characterised using election ionisation FT-ICR MS to reveal aromatic hydrocarbon and sulphur-containing compounds of increasing MW and increasing average number of aromatic rings per molecule (Fu et al., 2006). Five narrow, high boiling distillation cuts with nominal boiling ranges as narrow as 14°C were used to examine the characteristics of FDMS for the measurement of MW distributions (Qian et al., 2007). The mid-points of the MW distributions matched well with prior developed MW-BP correlations based on H/C ratio (Altgelt and Boduszynski, 1992), falling between the paraffins and alkyl-substituted phenanthrenes. Towards higher BPs, the fractions MW-BP behaviour obtained using FDMS approached that of tricyclic aromatic compounds. Since its introduction to the field of petroleomics, atmospheric pressure photo ionisation (APPI) has been widely used for the measurement of aromatic petroleum components (Purcell et al., 2006), even for a quantitative assessment of sulphur aromatic compounds in petroleum gas oils (Muller et al., 2012). Wang et al. (2016) used narrow distillation cuts (separated by 30°C nominal BP) from a vacuum gas oil to link compositional details obtained by APPI FT-ICR MS to the AEBP curves of the observed component families. Remarkably, the mass spectrometric compositional data led to semi-quantitative distillation curves, after calibration against simulated distillation. In another study, the distillation of biocrude and petroleum crude blends in conventional distillation units was recently assessed and matched with predicted behaviour (Ramirez et al., 2017). Cui et al. (2019) recently reported the characterisation of heteroatom compounds, mainly nitrogen-oxygen containing species, in a shale oil after fractionation of the oil into 15 narrow (20°C) distillation cuts and the light and heavy ends (<100°C and >400°C, respectively). The study reports details on the polar components, however the compositional information was not linked to the BP of the respective cuts.

In this study, we investigate a light and sour Arabian crude oil through fractionation by distillation into narrow boiling cuts, separated by approximately 16°C nominal boiling range. The 27 individual cuts cover the entire boiling range of the crude oil, including a light ends cut boiling below 149°C, and a final vacuum residue (VR) cut boiling above 566°C AEBP. Characterisation of the cuts was based on simulated distillation to assess the degree of overlap between adjacent cuts, determination of the MW distribution of the aromatic compounds by APPI mass spectrometry, and bulk parameters. The chemical and physical properties were also compared to predicted values using H/CAMS software.

## 2 Material and methods

Owing to the compositional complexity of the crude oil matrix, a fractionation by distillation following ASTM D2892 and D5236 methods was performed to obtain narrow distillation fractions (cuts) from the sour Arabian crude oil. Also, international standard methods (ASTM) and in-house methods were then employed for the characterisation of each distillation cut.

### 2.1 Crude oil

A commercial light, sour Arabian crude oil with the following bulk properties was selected for this study: gravity of 33.2° API, total sulphur content of 2.0% weight, wax content of 2.5% weight, total nitrogen content of 846 ppm weight and a low total acid number of 0.07 mg KOH per g of oil. The boiling distribution by simulated distillation (ASTM D7169) is provided in Table 1.

**Table 1** Crude oil BP curve by simulated distillation

| <i>Recovery [%weight]</i> | <i>Temperature [°C]</i> |
|---------------------------|-------------------------|
| IBP                       | -6                      |
| 5                         | 62                      |
| 10                        | 100                     |
| 20                        | 165                     |
| 30                        | 240                     |
| 40                        | 301                     |
| 50                        | 358                     |
| 60                        | 422                     |
| 70                        | 489                     |
| 80                        | 568                     |
| 90                        | 692                     |
| 95                        | n.d.                    |
| FBP                       | 720                     |

Notes: IBP = initial boiling point and FBP = final boiling point.

### 2.2 Chemicals

Toluene used for mass spectrometric analyses was procured from Sigma-Aldrich (Germany) at HPLC grade of  $\geq 99.9\%$  purity. ASTM specifications for the remaining solvents and purities were followed.

### 2.3 Fractionation

Fractionation of the crude oil samples into narrow boiling range cuts was performed using distillation according to ASTM D2892 for light and middle distillate cuts #1 to #15 and ASTM D5236 for heavy cuts #16 to #27. The first cut #1 was collected from IBP to 149°C, after which cuts with an equivalent BP range of 16°C were fractionated.

The distillation of the light cuts #1 to #4 ( $-43^{\circ}\text{C}$  to  $199^{\circ}\text{C}$ ) was performed at atmospheric pressure, the pressure for collecting cuts #5 to #11 ( $199^{\circ}\text{C}$  to  $316^{\circ}\text{C}$ ) was reduced to 100 mmHg, for cuts #12 to #15 ( $316^{\circ}\text{C}$  to  $382^{\circ}\text{C}$ ) to 2 mmHg, and finally for cuts #16 to #26 ( $382^{\circ}\text{C}$  to  $566^{\circ}\text{C}$ ) to 0.5 mmHg. Cut #27 is the vacuum distillation residue.

## 2.4 Characterisation

- *Physical properties:* the refractive index at  $25^{\circ}\text{C}$  and  $30^{\circ}\text{C}$  was determined according to ASTM D1218, the specific gravity according to ASTM D4052 and the density at  $16^{\circ}\text{C}$  ( $60^{\circ}\text{F}$ ) according to ASTM D4052. The boiling behaviour was assessed using simulated distillation (SIMDIS) for light and medium cuts (#1–#24) up to  $559^{\circ}\text{C}$  final AEBP according to ASTM D2887 and for heavy cuts (#25–#27) above  $441^{\circ}\text{C}$  initial AEBP according to ASTM D6352. The unfractionated crude oil was analysed according to ASTM D7169, which covers the hydrocarbons from C5 to C100, or equivalent to a boiling range up to  $720^{\circ}\text{C}$ .
- *Chemical properties:* total nitrogen content was determined according to ASTM D4629, the total sulphur content according to ASTM D4294. The group type quantification by gas chromatography into paraffins, isoparaffins, oxygenates, naphthenes and aromatics (PIONA) was conducted according to ASTM D6730, based on gas chromatography equipped with a 100 metre capillary column followed by flame ionisation detection. Quantitative  $^{13}\text{C}$  nuclear magnetic resonance (NMR) spectroscopy was performed according to ASTM D5292. Quantitative determination of the hydrogen content was performed according to a modified ASTM D4808 using a permanent magnet NMR spectrometer.

MW distributions of each cut were determined using an Agilent Technology G6230B time of flight mass spectrometer (TOF-MS) equipped with APPI source for the ionisation of aromatic hydrocarbons. Samples were shaken at 1,800 rpm for 30 s (fractions #20 and higher boiling) were heated to approximately  $50^{\circ}\text{C}$  beforehand before a sub-sample was taken and diluted to a final concentration of 0.1 mg per 1 g toluene. The diluted samples were delivered directly into the ion source via syringe pump at a flow rate of  $20\ \mu\text{l}\ \text{min}^{-1}$ . APPI furnace temperature was set to  $400^{\circ}\text{C}$  and drying gas temperature to  $300^{\circ}\text{C}$ , respectively. Nitrogen gas flow rate in the nebuliser was set to  $8\ \text{L}\ \text{min}^{-1}$  and the dry gas pressure to 40 psig, respectively. Ion source potentials were set to 3.0 kV for the capillary, fragmentor and skimmer to 150 V and 65 V, respectively. Ions were guided through an octapole with RF voltage at 750 Vpp. Mass spectra were collected from 100 m/z to 3,000 m/z, with approx. 9,900 transients averaged per spectrum ( $1\ \text{s}^{-1}$ ), accumulated for 1 min and finally summed into a single extracted mass spectrum (Masshunter software, Agilent Technologies). The peak threshold was manually adjusted to 200 (arbitrary unit) and the resulting peak list exported into Microsoft Excel to produce a summed mass spectral abundance curve (i.e., cumulative signal abundance vs. m/z).

## 2.5 Property prediction

H/CAMS Haverly crude assay and management software was used to predict cut yields and properties. For this purpose, the studied crude oil was entered with the accompanying standard crude assay parameters. Narrow cut points were then entered following the

experimental parameters, the crude oil virtually re-cut, and yields and properties predicted for each fraction.

## 2.6 Abbreviations

|                     |   |
|---------------------|---|
| <sup>13</sup> C NMR | Carbon-13 nuclear magnetic resonance                          |
| AEBP                | atmospheric equivalent boiling point                          |
| APPI                | atmospheric pressure photo ionisation                         |
| ASTM                | American society for testing and materials                    |
| BP                  | boiling point   |
| FDMS                | field desorption mass spectrometry                            |
| FT-ICR MS           | Fourier transform-ion cyclotron resonance mass spectrometry   |
| GCxGC               | comprehensive two-dimensional gas chromatography              |
| H/CAMS              | Haverly crude assay and management software                   |
| HPLC                | high performance liquid chromatography                        |
| MS                  | mass spectrometry   |
| MW                  | molecular weight  |
| PIONA               | paraffins, isoparaffins, oxygenates, naphthenes and aromatics |
| RF                  | radio frequency   |
| SIMDIS              | simulated distillation  |
| TOF-MS              | time of flight mass spectrometry                              |
| VR                  | vacuum residue.   |

## 3 Results and discussion

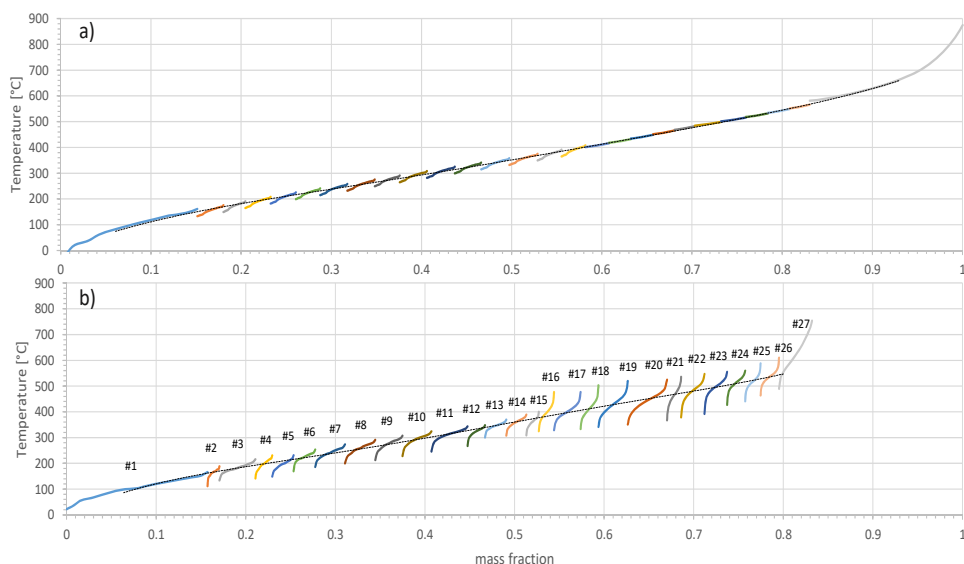
Following fractionation by distillation, the predicted and actual yields (volume and weight) are shown in Figures A1(a) and A1(b) (Appendix), respectively. Both datasets matched with the exception of a discrepancy in the heavy middle distillates region between roughly 300°C to 400°C mid-BPs. This discrepancy could be attributed to the fractionation conditions and yields. The distillation pressure is reduced to avoid residual oil cracking, first to 2 mmHg, while using the same thermal controls, then to 0.5 mmHg for the cuts boiling above 382°C. A limited condensate volume resulting from the narrow cut set points was also required to reduce the reflux ratio and fractionation take-off rates.

Due to the very narrow cut points for each fraction, a significant compositional overlap between consecutive fractions is expected. The overlap can be estimated using the simulated distillation curves (Figure 1). Figures 1(a) and 1(b) show the calculated and measured simulated distillation curves, respectively. The actual cuts have a significant overlap due to the fractionation conditions and the operational constraints of the distillation apparatus used (total capacity of 13 L required to produce sufficient yield for

each fraction). For cuts #16 and above, the boiling ranges of the individual fractions are expanded due to the necessary reduction of distillation pressure, as mentioned before (cuts above 316°C). Moreover, Figure 2 shows an expanded region of the measured simulated distillation curves. As is evident, significant overlap is expected between the narrow cuts and hence, adjacent cuts are expected to also have a significant compositional overlap. For example, the 0.95 mass fraction point of cut #7 overlaps with the 0.6 mass fraction point of cut #8. At the same time, it also overlaps with the 0.2 mass fraction point of cut #9. Twice removed cuts still have a significant overlap, e.g., the 0.95 mass fraction point of cut #7 overlaps with the 0.2 mass fraction point of cut #9 and even almost overlaps with the 0.1 mass fraction point of cut #10.

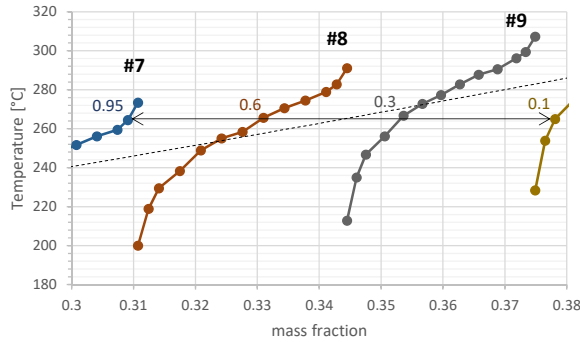
Despite the overlap between cuts, the average properties evolve as expected with the mid-BP of the cuts. Figure 3 shows a comparison of chemical and physical bulk properties between H/CAMS predictions and measured values for the actual cuts. Figure 3(a) shows the specific gravity by ASTM D4052 at 60°F, Figure 3(b) the refractive index by ASTM D1218 at 30°C, Figure 3(c) the mass fraction of total sulphur content by ASTM D4294, and Figure 3(d) the total nitrogen content by ASTM D4629 expressed as ppm (mass by mass part per million). The measured properties show slight bumps in the boiling range between 300°C and 400°C, corresponding to the changed distillation conditions remarked already in the yield discussion above. Besides these, the data curves are overall in good agreement with the predictions, indicating a successful fractionation by distillation.

**Figure 1** Simulated distillation curves by (a) H/CAMS prediction and (b) determined by ASTM D2887 and D6352 (see online version for colours)



Notes: The labels in (b) refer to the fraction cut number. The dashed lines represents the mid-point boiling curve of the whole crude oil.

**Figure 2** Detailed zoom of simulated distillation curves by ASTM D2887 showing the boiling range overlap between adjacent cuts (see online version for colours)



Notes: The relevant mass fractions are indicated in the colour of the corresponding cut in Figure 1. The dashed line represents the boiling distribution of the crude oil.

**Figure 3** Comparison between predicted properties of narrow distillation cuts using H/CAMS and measurement data for actual cuts for (a) specific gravity by ASTM D4052 at 60°F (b) refractive index by ASTM D1218 at 30°C (c) mass fraction of total sulphur content by ASTM D4294 and (d) total nitrogen content by ASTM D4629 expressed as ppm of mass (see online version for colours)

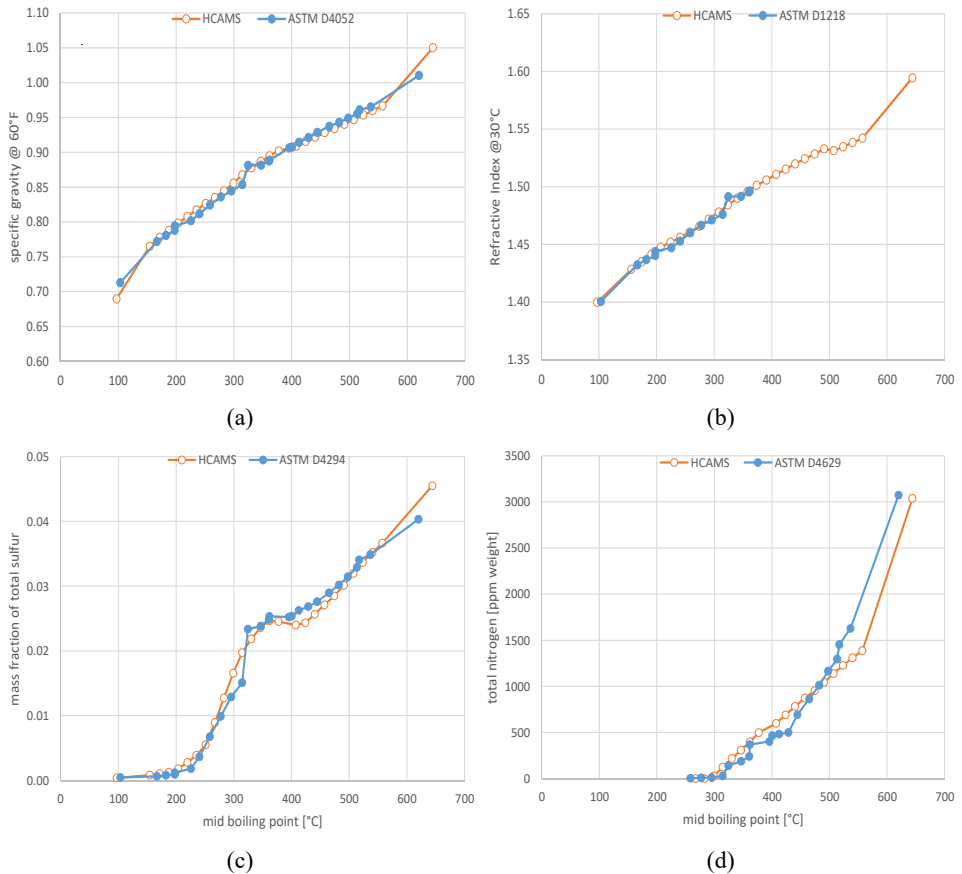


Photo-ionisation in combination with time of flight mass spectrometry allows, with some constraints, the direct measurement of a petroleum sample's MW distribution. The MW distributions obtained are limited to the aromatic components capable of undergoing photo ionisation. Although different aromatic species will have varying response factors depending on the extent of their aromatic system and molecular structure (Muller et al., 2012), a clear progression towards higher average MWs and widening MW distributions for higher boiling cuts can be observed. To use the mass spectral information, the relative cumulative abundance was summed from low to high  $m/z$  values (Figure A3, Appendix). The resulting MW distribution curves for consecutive distillation cuts are shown in Figure 4. The MW data reflects the overlap between fractions. The average MW curve for the crude oil is indicated as a dotted line in the graph.

The MW for each cut against its mid-BP is shown in Figure 5. The MW-BP curves for n-paraffins and PAH are indicated as green and red dotted lines, respectively. Average MW curves determined using APPI TOF-MS and predicted using H/CAMS software are shown as blue solid dots and orange hollow dots, respectively. Altgelt and Boduszynski (1992) developed a correlation between BP and MW, which includes the H/C ratio, equation (1) shown by brown diamonds in the Figure 5. This correlation is valid only for high boiling samples (Qian et al., 2007). The total hydrogen content of each cut was determined by NMR spectroscopy, and the carbon contents calculated as the mass balance of hydrogen, sulphur, and nitrogen (Figure A4, Appendix).

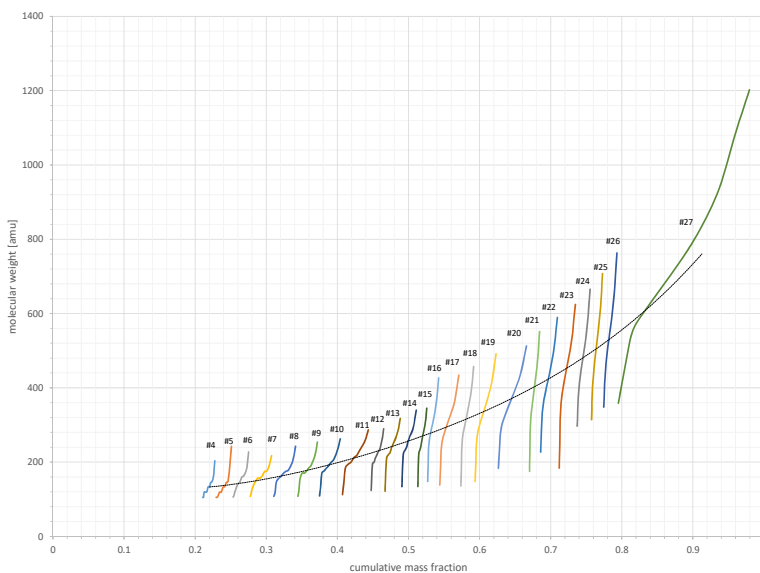
$$MW = 170 + 2.67 \times 10^{-7} \times BP^3 \times (H/C)^{0.9} \quad (1)$$

The H/CAMS predicted MWs up to a BP of 400°C exceed the ones of n-paraffins and then converge with the APPI TOF-MS MW-BP curve. The APPI TOF-MS MW-BP curve matches PAH components until approximately 300°C, and then converges with the H/CAMS predicted curve by 520°C. The deviation of the MS data can be explained by the selective ionisation of aromatic compounds. At lower MWs (corresponding to lower BPs) the present aromatic compounds are unsubstituted, or have few and short alkyl-substituents, hence pure PAH components dominate. Above 300°C BP, the presence of alkyl chains substituting the aromatic ring systems increases. Correspondingly, the aromatic compounds detectable by the APPI TOF-MS reflect better the average MW of the crude oil sample. Also, an increasing percentage of the molecules contains at least one aromatic ring, increasing the fraction of APPI amenable components in the higher boiling cuts to approximately 520°C where the MW-BP curves overlap. This indicates that the average molecular structure in the VR contains an aromatic group, and that the aromatic species constitute the crude oil MW distribution. The discussed APPI TOF-MS MW-BP curve is based on the mid-points of the SIMDIS BP curve and cumulative MW curve for each cut. Figure A5 (Appendix), shows further details that are useful to estimate the spread of the crude oil components in this graph. Curves for the intersections between 10% and 10% of SIMDIS BP curves and cumulative MW curves, and the 90% intersections are shown to provide an estimation of the spread of the petroleum composition and illustrated the associated uncertainty of this approach. The dotted lines above and below these 10% and 90% percentiles represent extreme cases where 90% MW intersect with 10% BP and, vice versa, where 90% BP intersects with 10% MW, respectively. In summary, the data indicates the importance of aromatic compounds for accurate MW-BP determination, whereby the average boiling behaviour

depends on the amount of aromatic components, as well as their degree of alkyl substitution.

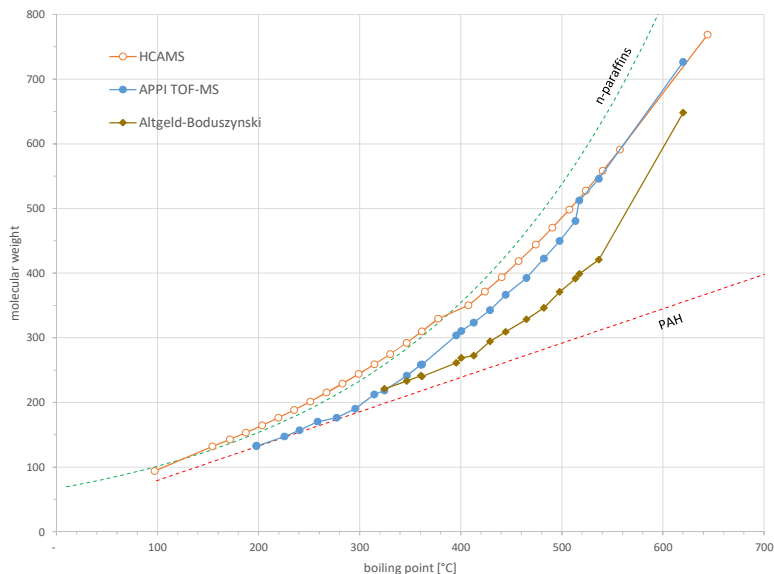
The evolution of aromatic compounds with the BP is also an important parameter to not only determine the process severity needed to refine the crude distillation fractions, but also ultimately the value of the crude oil. Furthermore, the H/C ratio was reported as the best input variable for modelling the BP-MW relation for whole crude oils and very high boiling atmospheric residue samples (Altgelt and Boduszynski, 1992). The predicted mass fraction of aromatic compounds is shown in Figure 6 alongside the aromatics content determined using PIONA analysis by gas chromatography. This technique is limited to low boiling fractions (cut #1 to #6) to the peak capacity of the instrument. Aromatics content across the entire boiling range of the crude oil can be accessed using quantitative carbon-13 nuclear magnetic resonance spectroscopy ( $^{13}\text{C}$  NMR). Based on their different chemical shifts, this method allows to determine the average ratio of carbon atoms located in aromatic rings to those in aliphatic groups (Figure 6, secondary axis). It is important to note that the aromatics content prediction and PIONA data account for the total mass fraction of aromatic molecules, which could be composed of unsubstituted or alkyl substituted aromatic ring systems (potentially including or excluding heteroatoms). In contrast, the  $^{13}\text{C}$  NMR data accounts directly for the carbon atoms present in aromatic rings; aliphatic groups substituting aromatic rings are accounted as aliphatic carbon atoms. Regardless of this difference, the derived aromatics trends in Figure 6 agree towards a local maximum of aromatic components from 180°C to 200°C, followed by a steady increase of aromatic components.

**Figure 4** MW vs. cumulative mass fractions determined using APPI TOF-MS (5% to 95% of the cumulative mass spectral abundances summed from low  $m/z$  to high  $m/z$  for each cut) (see online version for colours)



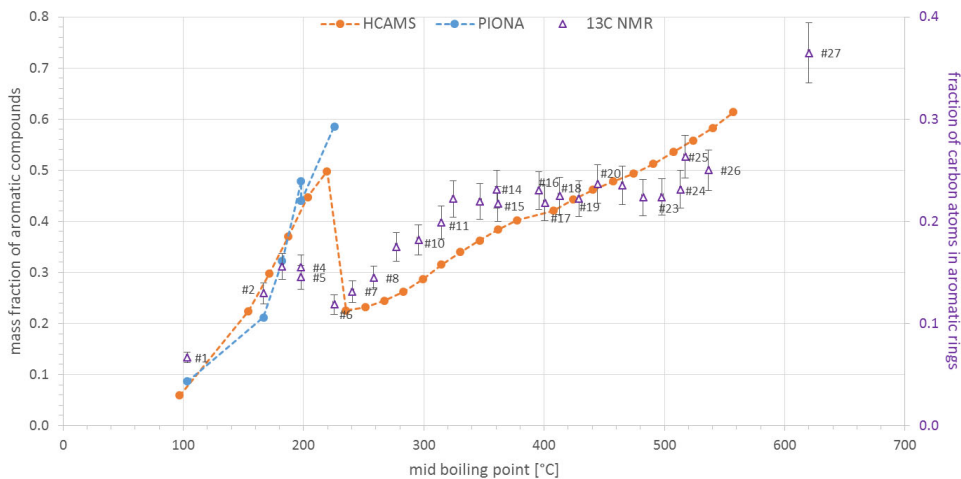
Notes: The labels in the graph refer to the fraction cut number, and the average MW curve for the crude oil is indicated as a dotted line.

**Figure 5** Average distribution of MW by APPI TOF-MS vs. BP by SIMDIS (●), and predicted values using H/CAMS (○) and Altgelt-Boduszynski's correlation (◆) (see online version for colours)



Notes: The MW-BP curves for n-paraffins and PAH are indicated as green and red dotted lines, respectively.

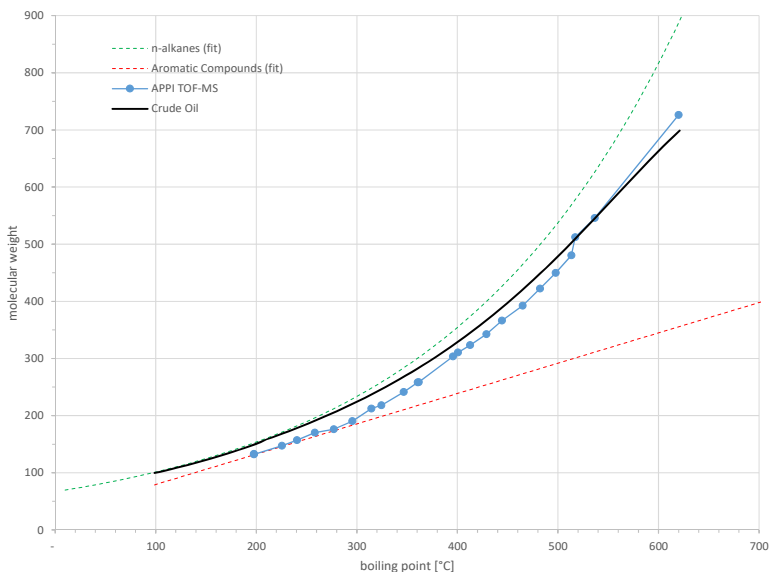
**Figure 6** Mass fraction of aromatic compounds in narrow distillation cuts by H/CAMS and PIONA (primary y-axis, left) (see online version for colours)



Notes: Overlaid is the fraction of carbon atoms in aromatic rings ( $\Delta$ ) determined using quantitative  $^{13}\text{C}$  NMR spectroscopy, with the percentage given on the secondary axis (right).

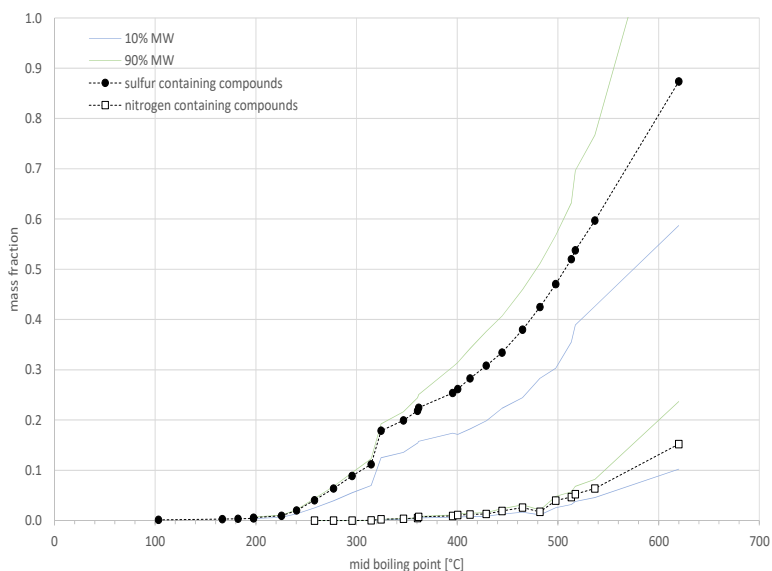
The MS data (Figure 5) indicated that the average crude oil BPs is determined by paraffins and aromatic components. The BP evolution of n-paraffins with increasing chain length is well known (Kudchadker and Zwolinski, 1966) and their correlation between MW and BP is known. At a similar BP, unsubstituted polycyclic aromatic hydrocarbons (PAH) have relatively lower MWs (Fu et al., 2006). The BP-MW relation for alkyl substituted aromatic compounds (and branched alkanes) depends on the exact molecular structure. Although isomers have varying BPs, their BPs mostly fall between those of n-paraffins and PAH with similar MW (Figure A6, Appendix) (Qian et al., 2007; Wang et al., 2016). Hence, the average petroleum molecules' MW to BP behaviour falls largely between those extremes. This is relevant especially for middle distillate fractions and heavier, where the compositional complexity is beyond the point to consider individual isomer's contributions. It was posited that using the average fraction of carbon atoms in aromatic rings and in aliphatic groups, as determined by  $^{13}\text{C}$  NMR, could provide a simpler way to better approximate the average BP-MW relation for the crude oil. The crude oil MW-BP curve based on the acquired  $^{13}\text{C}$  NMR data is represented by a black, solid line in the graph (Figure 7). The fit was determined by first approximating the BP evolution of the  $^{13}\text{C}$  NMR measured aromatics content (Figures A6 and A7, Appendix), and then weighting the data based on the assumption that more aliphatic carbon atoms (on average) relate to a 'more n-alkane-like' boiling behaviour, i.e., closer to the n-alkane curve in the plot (Figure 7) (Altgelt and Boduszynski, 1992). On the other hand, a higher fraction of carbon atoms in aromatic rings relate to a 'more aromatic-like' boiling behaviour, i.e., closer to the aromatic compounds line in this plot.

**Figure 7** BP vs. MW curve determined from the interpolation between n-paraffins and PAH using  $^{13}\text{C}$  NMR spectroscopy data (solid black line) (see online version for colours)



Note: The previously discussed APPI TOF-MS curve is shown for reference.

**Figure 8** Mass fraction of sulphur containing compounds (●) and nitrogen containing compounds (□) per BP in the crude oil calculated using the total sulphur content by ASTM D4294 and total nitrogen content by ASTM D4629, respectively, and the average MW distribution (see online version for colours)



Notes: Curves for 10% and 90% MW ranges are indicated for both heteroatom-containing compounds to estimate the possible ranges.

Using the cumulative distillation point method on the APPI TOF-MS data, the mid-point of the non-distillable VR fraction is found to be at  $m/z = 726$  (Figure A8, Appendix). In conjunction with the BP vs. MW curve, this gives an estimated AEBP of 620°C for the VR fraction. Consequently, this value is used as the final fractions mid-BP throughout this work.

Finally, with an average MW per BP curve established for the studied crude oil, the total sulphur and total nitrogen BP distributions [Figures 3(c) and 3(d)] were used to derive the average mass fractions of organo-sulphur and -nitrogen containing compounds (Figure 8). Calculation was based on the average MW (50% point) and 10% and 90% MW percentiles to estimate the spread of possible sulphur and nitrogen compound contents. With increasing heteroatom content and increasing average MW, the majority of molecules in high- and non-boiling fractions (boiling above AEBP 500°C) were found to contain a heteroatom. For the final VR cut of the studied crude oil, molecules on average contain at least one heteroatom, predominantly sulphur.

These findings have direct implications for molecular modelling efforts of sour crude oils, even for light crude oil such as the one reported here, to consider a majority of sulphur and/or sulphur/nitrogen containing aromatic compounds in the residue fractions. Consequently, the results show that pure PAH compounds are relatively rare in such oils.

## 4 Conclusions

In this study a light and sour Arabian crude oil was fractionated by distillation into narrow boiling cuts separated by approximately 16°C. The individual cuts were characterised using simulated distillation to assess the degree of overlap between adjacent cuts. Owing to the narrow temperature range of each cut, a significant overlap extending across three to four adjacent cuts was confirmed. The individual cuts were then characterised to establish the BP evolution of chemical and physical properties, which matched well overall with predicted values obtained using H/CAMS software, establishing that the fractionation by distillation had produced representative samples. APPI TOF-MS allowed measuring the MW distributions of the aromatic compounds present in each cut. For light and middle distillate cuts a deviation between the MS results and the predicted MW distributions by H/CAMS software is observed, and can be explained by the selective ionisation of aromatic compounds which omits the paraffin contribution to the MW distribution. For higher boiling cuts, with expectedly higher aromatic contents, the MW measurement and prediction converge.

Based on modelling MW-BP behaviour of pure n-alkanes and aromatic compounds, the average fraction of carbon atoms located in aromatic vs. aliphatic moieties, determined using quantitative <sup>13</sup>C NMR spectroscopy, allowed the calculation of the average MW-BP curve across the entire crude oil boiling range. The curve matches well with the experimental MS data for the heavy cuts, where sufficient aromatic compounds allow for the representative determination of MW distributions via photo-ionisation.

Finally, the MW-BP relation for the crude oil enabled the estimation of the equivalent mid-BP for the final VR cut, as well as an estimation of the mass fractions of the organo-sulphur and organo-nitrogen components, which were assessed through the combination of MW and heteroatom content distributions by BP. Above 500°C, the majority of compounds (i.e., more than half of the present molecules) seem to contain a sulphur atom. In the final VR cut boiling above 566°C (AEBP), most molecules contain one or more hetero atoms, indicating that pure hydrocarbon molecules, either saturated or aromatic, are rare.

## References

- Altgelt, K.H. and Boduszynski, M.M. (1992) 'Composition of heavy petroleums. 3. An improved boiling point-molecular weight relation', *Energy & Fuels*, Vol. 6, No. 1, pp.68–72.
- Boduszynski, M.M. (1987) 'Composition of heavy petroleums. 1. Molecular weight, hydrogen deficiency, and heteroatom concentration as a function of atmospheric pressure equivalent boiling point up to 1400°F (760°C)', *Energy & Fuels*, Vol. 1, No. 1, pp.2–11.
- Boduszynski, M.M. (1988) 'Composition of heavy petroleums. 2. Molecular characterization', *Energy & Fuels*, Vol. 2, No. 5, pp.597–613.
- Boduszynski, M.M. and Altgelt, K.H. (1992) 'Composition of heavy petroleums. 4. Significance of the extended atmospheric equivalent boiling point (AEBP) scale', *Energy & Fuels*, Vol. 6, No. 1, pp.72–76.
- Cui, D., Wang, Q., Wang, Z.C., Liu, Q., Pan, S., Bai, J. and Liu, B. (2019) 'Compositional analysis of heteroatom compounds in Huadian shale oil using various analytical techniques', *Energy & Fuels*, Vol. 33, No. 2, pp.946–56.

- Fu, J., Kim, S., Rodgers, R.P., Hendrickson, C.L. and Marshall, A.G. (2006) 'Nonpolar compositional analysis of vacuum gas oil distillation fractions by electron ionization Fourier transform ion cyclotron resonance mass spectrometry', *Energy & Fuels*, Vol. 20, No. 2, pp.661–667.
- Han, Y., Zhanga, Y., Xua, C. and Hsu, C.S. (2018) 'Molecular characterization of sulfur containing compounds in petroleum', *Fuel*, Vol. 221, pp.144–158.
- Kudchadker, A.P. and Zwolinski, B.J. (1966) 'Vapor pressures and boiling points of normal alkanes, C<sub>21</sub> to C<sub>100</sub>', *Journal of Chemical and Engineering Data*, Vol. 11, No. 2, pp.253–255.
- Muller, H., Adam, F.M., Panda, S.K., Al-Jawad, H.H. and Al-Hajji, A.A. (2012) 'Evaluation of quantitative sulfur speciation in gas oils by Fourier transform ion cyclotron resonance mass spectrometry: validation by comprehensive two-dimensional gas chromatography', *Journal of the American Society for Mass Spectrometry*, Vol. 23, No. 5, pp.806–815.
- Nedelchev, A., Stratiev, D., Ivanov, A. and Stoilov, G. (2011) 'Boiling point distribution of crude oils based on TBP and astm D-86 distillation data', *Petroleum and Coal*, Vol. 53, pp.275–290.
- Purcell, J.M., Hendrickson, C.L., Rodgers, R.P. and Marshall, A.G. (2006) 'Atmospheric pressure photoionization Fourier transform ion cyclotron resonance mass spectrometry for complex mixture analysis', *Analytical Chemistry*, Vol. 78, No. 16, pp.5906–5912.
- Qian, K., Edwards, K.E., Siskin, M., Olmstead, W.N., Mennito, A.S., Dechert, G.J. and Hoosain, N.E. (2007) 'Desorption and ionization of heavy petroleum molecules and measurement of molecular weight distributions', *Energy & Fuels*, Vol. 21, No. 2, pp.1042–1047.
- Ramirez, J.A., Brown, R.J. and Rainey, T.J. (2017) 'Liquefaction biocrudes and their petroleum crude blends for processing in conventional distillation units', *Fuel Processing Technology*, Vol. 167, pp.674–83.
- Rodgers, R.P. and McKenna, A.M. (2011) 'Review: petroleum analysis', *Analytical Chemistry*, Vol. 83, pp.4665–87.
- Sama, S.G., Farenc, M., Barrère-Mangote, C., Lobinski, R., Afonso, C., Bouyssière, B. and Giusti, P. (2018) 'Review: molecular fingerprints and speciation of crude oils and heavy fractions', *Energy & Fuels*, Vol. 32, No. 4, pp.4593–4605.
- Wang, W., Liu, Y., Liu, Z. and Tian, S. (2016) 'Detailed chemical composition of straight-run vacuum gas oil and its distillates as a function of the atmospheric equivalent boiling point', *Energy & Fuels*, Vol. 30, No. 2, pp.968–974.

## Appendix

The n-alkanes were fit with an exponential function ( $MW = a * \exp(BP * b)$ ) and the aromatic hydrocarbons with a linear fit ( $MW = a * BP + b$ ); coefficients are provided in the Table 2. The fraction of carbon atoms in aromatic groups at a given BP ( $C_{aro}$ , see Figure A7) was used to approximate the contributions of n-alkane and aromatic hydrocarbons functions according to equation (A1).

$$MW_{crude} = MW_{n-alkanes} \times (1 - C_{aro}) + MW_{aromatic\ hydrocarbons} \times C_{aro} \quad (A1)$$

**Table 2** Coefficients for fitting pure components

|   | <i>n-alkanes</i> | <i>Aromatic hydrocarbons</i> |
|---|------------------|------------------------------|
| a | 6.67E+01         | 5.31E-01                     |
| b | 4.17E-03         | 2.63E+01                     |

**Figure A1** Cumulative yield curves for narrow distillation cuts predicted using H/CAMS and actual fractions for, (a) volume (b) weight recovered (see online version for colours)

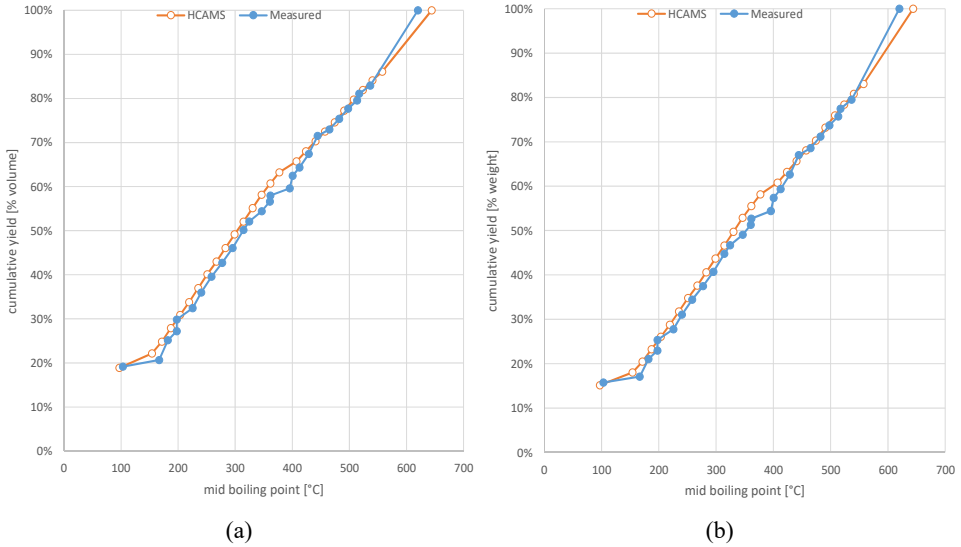


**Figure A2** APPI TOF-mass spectra for narrow distillation cuts

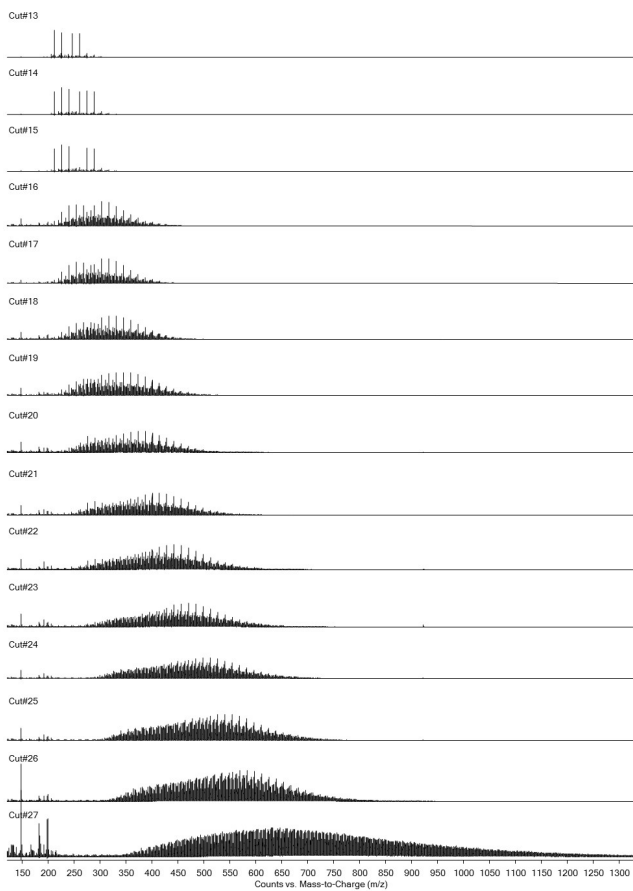
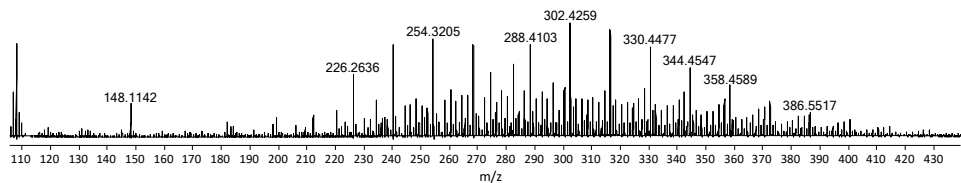
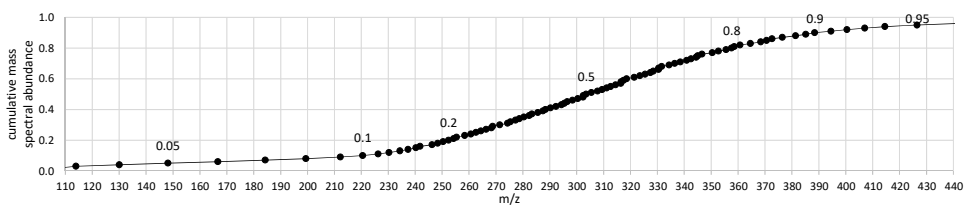


**Figure A3** (a) APPI TOF-mass spectrum for narrow distillation cut #16 (b) Cumulative relative mass spectral abundance across the sample  $m/z$  range

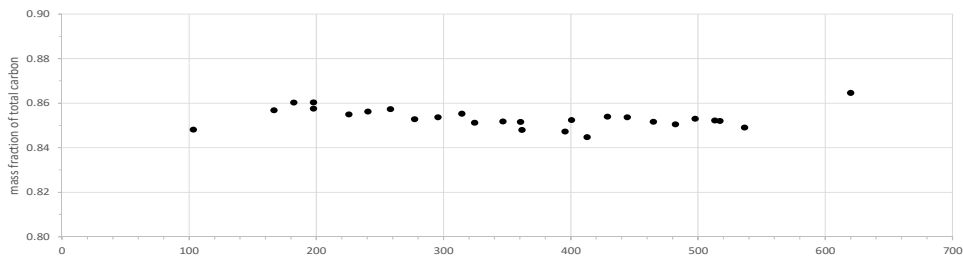


(a)

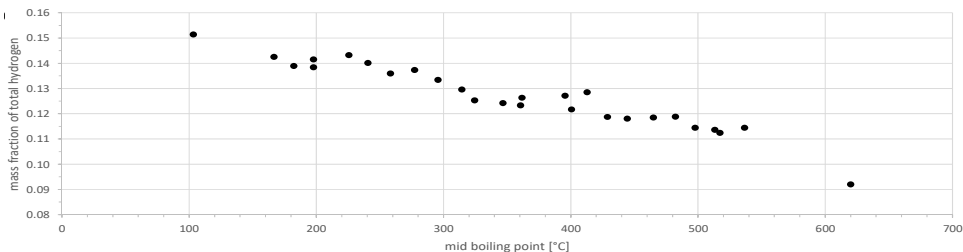


(b)

**Figure A4** Total (a) carbon (b) hydrogen contents as mass fractions per average BP

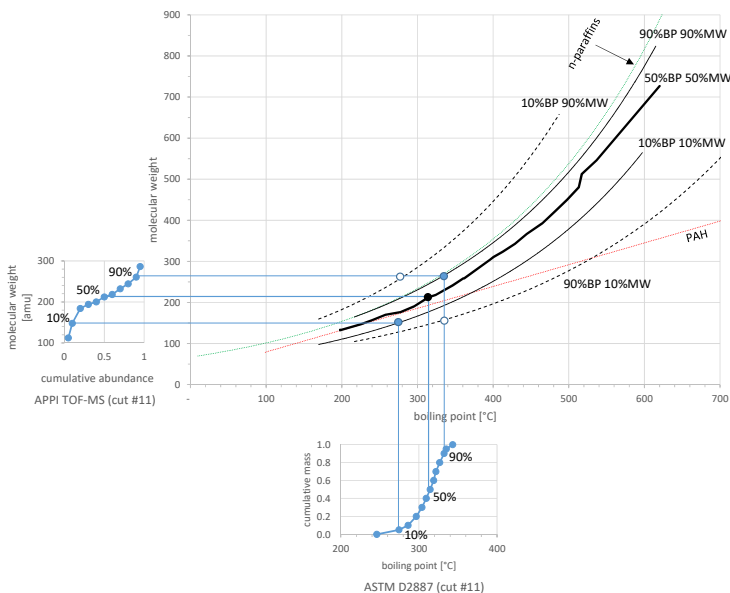


(a)

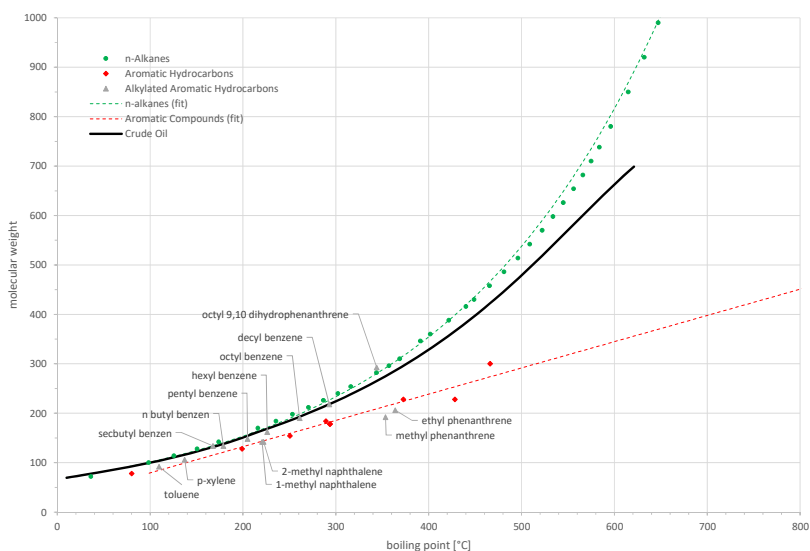


(b)

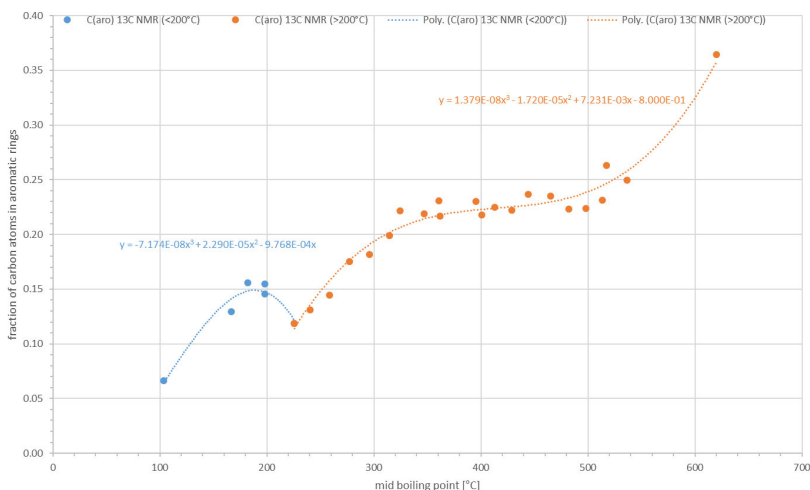
**Figure A5** Explanation of the uncertainty of the cumulative MW distributions by APPI TOF-MS vs. BP by SIMDIS (see online version for colours)



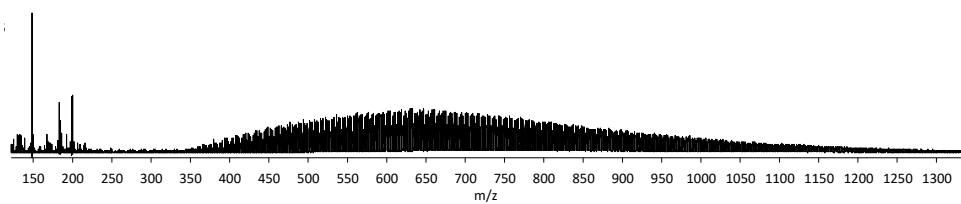
Notes: The centre line shows the median where 50% MW intersects with the 50% BP for each cut (thick solid line). Above and below the median line are the 90% and 10% curves, respectively, where the 90% BP and MW values, and the 10% BP and MW values intersect. The dotted lines above and below these represent an extreme case where 90% MW intersect with the 10% BP and the 90% BP intersects with 10% MW, respectively.

**Figure A6** Average distribution of MW vs. BP for n-alkanes (green dotted line), aromatic hydrocarbons (red dotted line) (see online version for colours)

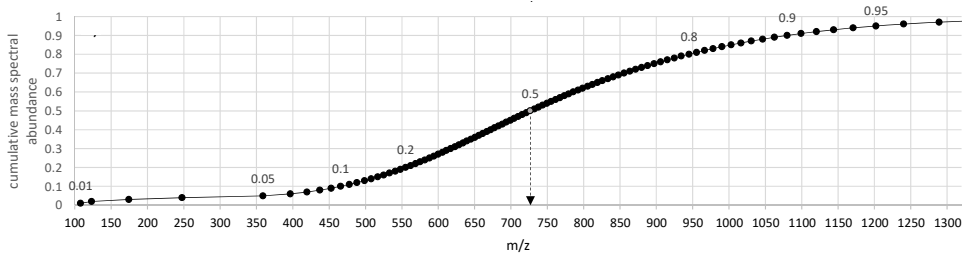
Notes: Individual alkyl-aromatic compounds are identified for comparison ( $\blacktriangle$ ). Values for the crude oil (solid black line) were calculated from the linear interpolation between the n-alkanes fit and the aromatic compounds fit using as a weighting factor the fraction of carbon atoms in aromatic rings by  $^{13}\text{C}$  NMR spectroscopy data.

**Figure A7** Polynomial fits for the fraction of carbon atoms in aromatic rings determined using  $^{13}\text{C}$  NMR spectroscopy (see online version for colours)

Notes: Two distinct regions in the plot, cuts boiling below 210°C and cuts boiling above 210°C, were fitted with the 3rd order polynomial equations provided in the graph. These functions together provide a continuous distribution of the fraction of carbon atoms in aromatic vs. aliphatic groups ( $C_{\text{aro}}$ ) across the relevant boiling range.

**Figure A8** (a) APPI TOF-mass spectrum for narrow distillation cut #27 (b) Cumulative relative mass spectral abundance across the sample  $m/z$  range

(a)



(b)

Note: The 0.5 cumulative abundance point is marked and corresponds to  $m/z = 726$ .